ELectronics EXpress

IEICE Electronics Express, Vol.1, No.17, 528–533

Alternative formulation of three dimensional frequency dependent ADI-FDTD method

Fumie Costen[a)] **and Arnaud Thiry**[b)]

School of Computer Science, The University of Manchester, Oxford Road, Manchester, M13 9PL, UK

a) *fumie.costen@manchester.ac.uk*

b) *arnaud.thiry@cs.man.ac.uk*

Abstract: An alternative formulation for a frequency dependent (FD) ADI-FDTD method is proposed, based on an electric flux field **D** tridiagonal matrix rather than an electric field matrix. The procedure for **D** source excitation is explained. Results show that the accuracy of the method is unaffected by the inclusion of frequency dependency in the model, compared with FD-FDTD.

Keywords: electromagnetic propagation in dispersive media, FDTD methods, transient propagation, Alternating-Direction Implicit technique, electric flux field source excitation, electric flux field absorbing boundary condition

Classification: Electromagnetic theory

References

[1] T. Namiki, "A new FDTD algorithm based on alternating-direction implicit method," *IEEE Trans. Microwave Theory Tech.*, vol. 47, pp. 2003–2007, 1999.

[2] S. W. Staker, C. L. Holloway, A. U. Bhobe, and M. Piket-May "Alternating-direction implicit (ADI) formulation of the finite-differencetime-domain (FDTD) method: Algorithm and material dispersion imple-mentation," *IEEE Trans. Electromagn. Compat.*, vol. 45, pp. 156–166, 2003.

[3] C. L. Holloway, P. M. McKenna, R. A. Dalke, R. A. Perala, and C. L. Devor, Jr., "Time-domain modeling, characterization, and measurements of anechoic and semi-anechoic electromagnetic test chambers," *IEEE Trans. Electromagn. Compat.*, vol. 44, pp. 102–118, 2002.

[4] C. Yuan and Z. Chen, "On the modeling of conducting media with the unconditionally stable ADI-FDTD method," *IEEE Trans. Microwave Theory Tech.*, vol. 51, no. 8, pp. 1929–1938, 2003.

[5] S. G. Garcia, R. G. Rubio, A. R. Bretones, and R. G. Martin, "Extension of the ADI-FDTD method to Debye media," *IEEE Trans. Antennas Propagat.*, vol. 51, no. 11, pp. 3183–3186, 2003.

[6] S. Schmidt and G. Lazzi, "Extension and validation of a perfectly matched layer formulation for the unconditionally stable D-H FDTD method," *IEEE Microwave Wireless Comp. Lett.*, vol. 13, pp. 345–347, 2003.

DOI: 10.1587/elex.1.528
Received October 29, 2004
Accepted November 08, 2004
Published December 10, 2004

[7] F. Costen, "A proposal of 3D frequency dependent ADI-FDTD with conductive loss," *Int. Conf. Comput. Electromagn.*, pp. 169–170, 2004.
[8] X. T. Dong, N. V. Venkatarayalu, B. Guo, W. Y. Yin, and Y. B. Gan, "General formulation of unconditionally stable ADI-FDTD method in linear dispersive media," *IEEE Trans. Microwave Theory Tech.*, 2004.

1 Introduction

In recent years, the Alternating Direction Implicit (ADI) method has been introduced to the Finite Difference Time Domain method (FDTD) [1]. The standard explicit FDTD has to satisfy the Courant-Friedrichs-Lewy (CFL) bound to be stable. Cases requiring small spatial discretization lead to excessive time sampling and increase the total CPU time required in FDTD. On the other hand, ADI-FDTD is unconditionally stable when taking sampling times greater than the limit set by the CFL condition, so keeping the total elapsed time within a practical time range. Thus ADI-FDTD is attractive when, for example, studying the influence of skin effects in conductive materials or signal reflections in lossy media for microwave imaging with UltraWideBand (UWB) systems. These UWB systems typically have frequency dependent lossy media parameters but ADI-FDTD and FDTD have the media parameters constant across frequencies. Adaptation of ADI-FDTD to such dispersive environments is required to accommodate UWB systems.

Holloway *et al* [2, 3] accounted for material dispersion in the magnetic field and mentioned the possibility of dealing with material dispersion in the electric field. However, [2] and [3] do not give an implementation of ADI-FDTD which deals with material with frequency dependent (FD) permittivity ϵ and ohmic losses. Chen *et al* 's [4] concern focuses on conductive materials. Garcia *et al* [5] deal with the Debye model utilizing the electrical polarization vector field. This paper describes an alternative technique with the electric flux density $\mathbf{D}$, similar to the work by Lazzi *et al* [6], but with FD materials for UWB systems. This runs parallel to [5] and provides convergent evidence for the general approach to FD materials in ADI-FDTD class problems. The novelty of this paper is in proposing an FD-ADI-FDTD which can deal with Debye dispersive materials with ohmic losses, along with the solutions to the problems on the $\mathbf{D}$ source excitation.

2 Numerical formulation

2.1 Tridiagonal matrix for electric flux field calculation

FD-ADI-FDTD is based on Faraday's law, Ampere's law, as is the case in [6], and the relationship between $\mathbf{D}$ and the electric field $\mathbf{E}$ with ϵ. When the first order Debye model for FD media is utilized, the relative permittivity ϵ_r is expressed as $\epsilon_r = \epsilon_\infty + \dfrac{\epsilon_S - \epsilon_\infty}{1 + \jmath\omega\tau_D}$ where ϵ_∞, ϵ_S, and τ_D are optical permittivity, static permittivity, and the relaxation time, respectively. Thus, taking the conductivity σ into account, $\mathbf{D} = \left(\epsilon_0\epsilon_\infty + \dfrac{\epsilon_0\epsilon_S - \epsilon_0\epsilon_\infty}{1 + \jmath\omega\tau_D} - \jmath\dfrac{\sigma}{\omega}\right)\mathbf{E}$ where

DOI: 10.1587/elex.1.528
Received October 29, 2004
Accepted November 08, 2004
Published December 10, 2004

ϵ_0 is the permittivity of free space. Here, the term of $\frac{\sigma}{j\omega}$ yields the term $(j\omega)^2$. This makes the implementation of FD-ADI-FDTD more complicated than that proposed elsewhere [2], which does not take into account the ohmic losses. The relationship between $\mathbf{D}$ and $\mathbf{E}$ above is re-written as a differential equation: $\tau_{\mathrm{D}}\frac{\partial^2\mathbf{D}}{\partial t^2}+\frac{\partial\mathbf{D}}{\partial t}=\epsilon_0\epsilon_\infty\tau_{\mathrm{D}}\frac{\partial^2\mathbf{E}}{\partial t^2}+(\epsilon_0\epsilon_{\mathrm{S}}+\sigma\tau_{\mathrm{D}})\frac{\partial\mathbf{E}}{\partial t}+\sigma\mathbf{E}$ which is discretized by the central difference approximation. The Crank-Nicolson scheme is applied to the full partial differential equation system given by the Maxwell curl equations, $\nabla\times\mathbf{E}=-\mu\frac{\partial\mathbf{H}}{\partial t}$ and $\nabla\times\mathbf{H}=\frac{\partial\mathbf{D}}{\partial t}$, where $\mathbf{H}$ is the magnetic field. They are then turned into the following two half steps scheme by the Peaceman-Rachford-Douglas technique. The first half step of $H_{y(i,j,k)}$ and $D_{x(i,j,k)}$ is written as $\mu\frac{H_y^{n+\frac{1}{2}}(i,j,k)-H_y^n(i,j,k)}{\frac{1}{2}\Delta t}=\frac{E_z^n(i,j,k)-E_z^n(i-1,j,k)}{\Delta x}-\frac{E_x^{n+\frac{1}{2}}(i,j,k)-E_x^{n+\frac{1}{2}}(i,j,k-1)}{\Delta z}$ and $\frac{D_x^{n+\frac{1}{2}}(i,j,k)-D_x^n(i,j,k)}{\frac{1}{2}\Delta t}=\frac{H_z^n(i,j+1,k)-H_z^n(i,j,k)}{\Delta y}-\frac{H_y^{n+\frac{1}{2}}(i,j,k+1)-H_y^{n+\frac{1}{2}}(i,j,k)}{\Delta z}$ where Δt is the temporal discretization and the uniform spatial discretization of Δx, Δy and Δz has the value of Δs. Numerical manipulation of these two equations together with the central difference approximation of the differential equation of the relationship between $\mathbf{D}$ and $\mathbf{E}$ leads to $f_{1k}D_x^{n+\frac{1}{2}}(i,j,k+1)+f_{2k}D_x^{n+\frac{1}{2}}(i,j,k)+f_{3k}D_x^{n+\frac{1}{2}}(i,j,k-1)=f_{4k}$ for $k_{min}+1\le k\le k_{max}-1$ where f_{1k}, f_{2k}, and f_{3k} consist of the media parameters exclusively, whilst f_{4k} consists of a combination of $\mathbf{D}^n$, $\mathbf{D}^{n-\frac{1}{2}}$, $\mathbf{E}^n$, $\mathbf{E}^{n-\frac{1}{2}}$, $\mathbf{H}^n$ as well as media parameters. $k-2$ equations from this equation and two equations for $k=k_{min}$ and k_{max} from the boundary condition form a k_{max} dimensional tridiagonal matrix to solve $\mathbf{D}^{n+\frac{1}{2}}$. $\mathbf{D}^{n+\frac{1}{2}}$ gives $\mathbf{E}^{n+\frac{1}{2}}$ through the relationship between $\mathbf{D}$ and $\mathbf{E}$. $\mathbf{E}^{n+\frac{1}{2}}$ is utilized for the calculation of $\mathbf{H}^{n+\frac{1}{2}}$. The remaining equations for the rest of the field components and for the second half step can be easily deducted by a permutation of indexes. More details on the major updating equations used for FD-ADI-FDTD can be found in [7]. [Note Δt in equations in [7] needs to be replaced by $\Delta t/2$.]

2.2 Source excitation in lossy media

In FD-FDTD, the source excitation is carried out at $\mathbf{E}_z$. In FD-ADI-FDTD, all fields are concomitant, so the source excitation needs to be embedded into the tridiagonal matrix which solves $\mathbf{D}$ to keep the symmetry of the system. In lossy media, the waveforms of $\mathbf{E}$ and $\mathbf{D}$ at the source location are different. If the waveform, which is used for the source excitation in FD-FDTD, is utilized for the $\mathbf{D}$ field excitation in FD-ADI-FDTD, the waveforms received from these two schemes mismatch; Thus accuracy assessment of FD-ADI-FDTD compared with FD-FDTD becomes impossible. Therefore, the $\mathbf{D}$ field excitation must be dealt with in an appropriate manner. Assume FD-FDTD excites a point source at (i_S,j_S,k_S) with $E_{z_{SF}}^n$ at each time step. The $\mathbf{D}_z$ field source excitation $D_{z_{SA}}^n$ in FD-ADI-FDTD, equivalent to the $\mathbf{E}_z$ field excitation in FD-FDTD, is carried out using the recurrence relation with FD-FDTD excitation $E_{z_{SF}}^n$: $D_{z_{SA}}^{n+\frac{1}{2}}=$

DOI: 10.1587/elex.1.528
Received October 29, 2004
Accepted November 08, 2004
Published December 10, 2004

$\frac{a_{4S}}{a_{1S}}E_{z_{S^F}}^{n+\frac{1}{2}} + \frac{a_{5S}}{a_{1S}}E_{z_{S^F}}^{n} + \frac{a_{6S}}{a_{1S}}E_{z_{S^F}}^{n-\frac{1}{2}} - \frac{a_{2S}}{a_{1S}}D_{z_{S^A}}^{n} - \frac{a_{3S}}{a_{1S}}D_{z_{S^A}}^{n-\frac{1}{2}}$ where $a_{1S} = \frac{\tau_{\mathrm{D}(i_S,j_S,k_S)}}{(\frac{1}{2}\Delta t)^2} + \frac{1}{(\frac{1}{2}\Delta t)}, a_{3S} = \frac{\tau_{\mathrm{D}(i_S,j_S,k_S)}}{(\frac{1}{2}\Delta t)^2}, a_{2S} = -2a_{3S} - \frac{1}{(\frac{1}{2}\Delta t)}, a_{5S} = -a_{4S} - a_{6S} + \sigma_{(i_S,j_S,k_S)}, a_{4S} = a_{6S} + \frac{\epsilon_0\epsilon_{\mathrm{S}(i_S,j_S,k_S)} + \sigma_{(i_S,j_S,k_S)}\tau_{\mathrm{D}(i_S,j_S,k_S)}}{(\frac{1}{2}\Delta t)} + \frac{\sigma_{(i_S,j_S,k_S)}}{2}$, $a_{6S} = \epsilon_0\epsilon_{\infty(i_S,j_S,k_S)}a_{3S}$. This derives from the equation of relationship between $\mathbf{D}$ and $\mathbf{E}$ shown at the beginning of Sec. 2.1.

3 Computational requirements

3.1 Memory requirement

Generally, ADI-FDTD is reported as having higher memory requirements than explicit FDTD. However, this is not the case for FD-FDTD and FD-ADI-FDTD. When FD-ADI-FDTD is implemented straight from the equation, it needs to store $\mathbf{D}^{n+\frac{1}{2}}$, $\mathbf{D}^{n}$, $\mathbf{D}^{n-\frac{1}{2}}$, $\mathbf{E}^{n+\frac{1}{2}}$, $\mathbf{E}^{n}$, $\mathbf{E}^{n-\frac{1}{2}}$, $\mathbf{H}^{n+\frac{1}{2}}$, $\mathbf{H}^{n}$. However, both $\mathbf{E}^{n+\frac{1}{2}}$ and $\mathbf{E}^{n-\frac{1}{2}}$ are never used together to calculate other field values. Thus, a single variable can be used for both $\mathbf{E}^{n+\frac{1}{2}}$ and $\mathbf{E}^{n-\frac{1}{2}}$ and the same for $\mathbf{H}^{n+\frac{1}{2}}$ and $\mathbf{H}^{n}$. $\mathbf{E}^{n+\frac{1}{2}}$ becomes a function of $\mathbf{D}^{n+\frac{1}{2}}$, $\mathbf{D}^{n}$, $\mathbf{D}^{n-\frac{1}{2}}$, $\mathbf{E}^{n}$, $\mathbf{E}^{n\pm\frac{1}{2}}$. Equivallently, $\mathbf{H}^{n+\frac{1}{2}}$ becomes a function of $\mathbf{E}^{n}$, $\mathbf{E}^{n+1}$ and $\mathbf{H}^{n(+\frac{1}{2})}$. In this way, FD-ADI-FDTD requires memory space for $\mathbf{D}^{n+\frac{1}{2}}$, $\mathbf{D}^{n}$, $\mathbf{D}^{n-\frac{1}{2}}$, $\mathbf{E}^{n\pm\frac{1}{2}}$, $\mathbf{E}^{n}$, $\mathbf{H}^{n(+\frac{1}{2})}$. The same analysis on FD-FDTD implementation gives $\mathbf{D}^{n+1}$, $\mathbf{D}^{n}$, $\mathbf{D}^{n-1}$, $\mathbf{E}^{n\pm1}$, $\mathbf{E}^{n}$, $\mathbf{H}^{n(+1)}$. Obviously, the FD-ADI-FDTD and FD-FDTD calculation procedures differ. FD-ADI-FDTD needs more memory than FD-FDTD for the tridiagonal matrix for $\mathbf{D}$ field calculation. However, this matrix is decomposed into three k_{max}-dimensional vectors. Compared with field storage for the whole calculation space, this requirement is trivial. Thus there is no noticeable increase in memory. A similar discussion on memory requirement is presented in [8].

3.2 CPU time usage

The elapsed time ratios between FD-FDTD and FD-ADI-FDTD (fitted curve $2.3 + N^{0.14}$) and between ADI-FDTD and FD-ADI-FDTD (fitted curve $N^{0.03}$) are shown in Fig. 1. The machine used for calculation is equipped with AMD Athlon™ XP 2000+ with 512 MB of memory. This reveals that the frequency dependency is included in ADI-FDTD within a 39% average increase

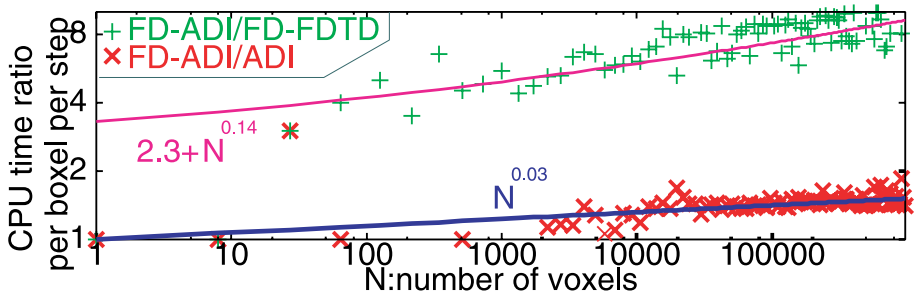

Fig. 1. The computational time ratio of FD-ADI-FDTD against FD-FDTD and ADI-FDTD

DOI: 10.1587/elex.1.528
Received October 29, 2004
Accepted November 08, 2004
Published December 10, 2004

in CPU time requirement, and that when $N = 10^5$, if Δt in FD-ADI-FDTD is 6 or more times larger than the Δt of FD-FDTD, FD-ADI-FDTD is faster.

4 Verification

4.1 Stability

In first order Debye dispersive materials with ohmic losses, a complex relative permittivity is expressed as $\left(\epsilon_\infty + \frac{\epsilon_S - \epsilon_\infty}{1+(\omega\tau_D)^2} - \jmath\left\{\frac{\sigma}{\omega\epsilon_0} + \frac{\omega\tau_D(\epsilon_S-\epsilon_\infty)}{1+(\omega\tau_D)^2}\right\}\right)$. Each frequency component has its own propagation speed and the highest propagation speed v_h is limited by the speed of light v. The CFL stability condition becomes $\Delta t \le \Delta s/(\sqrt{3}v_h) = \Delta s/(\sqrt{3}v) \times (v/v_h)$. This implies that the maximum Δt possible in FD-FDTD for a lossy case, defined as $\Delta t_{\mathrm{CFLlossy}}$, increases compared with the lossless case ($\Delta t_{\mathrm{CFLlossless}}$) by v/v_h.

Stability in FD-ADI-FDTD is verified numerically by receiving UWB signals in an exemplary lossy medium with (ϵ_S, ϵ_∞, σ, τ_D) = (57.6, 4.5, 0.7 S/m, 7 ps). The transmitter is located at the center of a 150 Δs cubic calculation space. Δs is set to $\lambda_{7\,\mathrm{GHz,vac.}}/90 = 4.76 \times 10^{-4}$ m where $\lambda_{7\,\mathrm{GHz,vac.}}$ is the wavelength of the continuous wave at 7 GHz. The mainlobe in the frequency spectrum of the source excitation terminates around 25 GHz. By 50 GHz, the spectrum shows −60 dB attenuation; The energy above this frequency can be regarded as a minor fraction of the pulse. The propagation speed at 50 GHz is used as v_h to determine $\Delta t_{\mathrm{CFLlossy}}$. As the relative permittivity of the medium at 50 GHz is $13.6 + \jmath 20.3$, v_h becomes $v/\sqrt{13.6}$ which results in $\Delta t_{\mathrm{CFLlossy}} = \sqrt{13.6}\ \Delta t_{\mathrm{CFLlossless}} = 3.3$ ps. Therefore, FD-FDTD should be stable at $\Delta t_{\mathrm{CFLlossy}} = 3.3$ ps. In this paper, $\Delta t/\Delta t_{\mathrm{CFLlossy}}$ and $\Delta t/\Delta t_{\mathrm{CFLlossless}}$ are called the CFL Number (CFLN) N_{CFL} for lossy and lossless cases, respectively.

Fig. 2 shows the signals received 15 Δs away from the source for N_{CFL} = 1 and 2 before any boundary reflection reaches the receiver as in a free space simulation. The signals coincide for $N_{CFL} = 1$. FD-ADI-FDTD shows its stability with $N_{CFL} = 2$ whilst FD-FDTD becomes unstable and diverges. Stability for FD-ADI-FDTD is observed when $N_{CFL} > 1$ with a variety of media parameters.

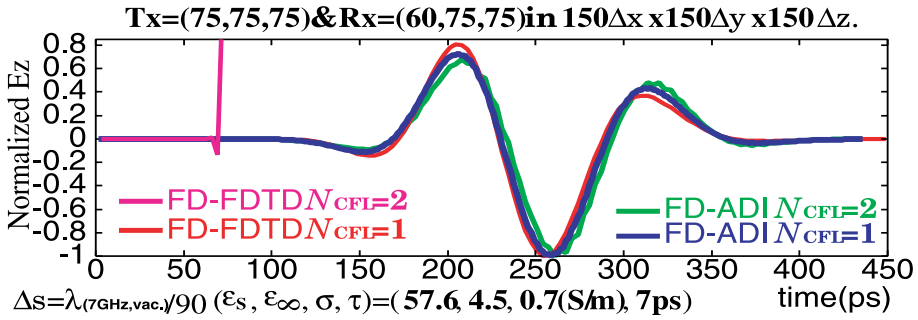

Fig. 2. UWB signals received in a lossy medium

DOI: 10.1587/elex.1.528
Received October 29, 2004
Accepted November 08, 2004
Published December 10, 2004

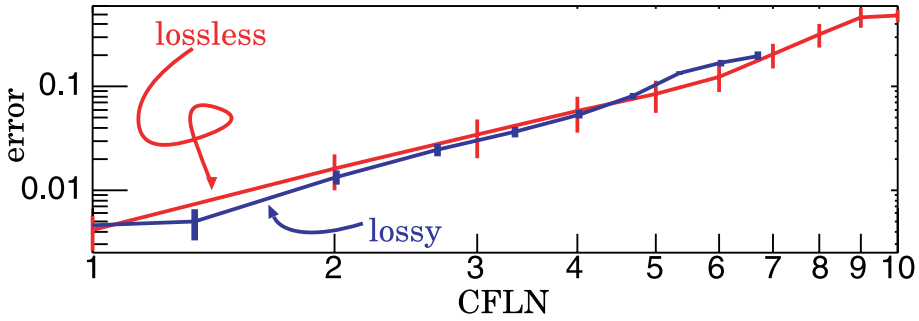

Fig. 3. The error from FD-ADI-FDTD and FD-FDTD. The vertical lines are 95% confidence intervals on an assumption of normality.

4.2 Accuracy

Although there is no stability constraint on Δt, there is an influence on accuracy. The accuracy is measured by UWB excitation in a radio environment with voxel number and size the same as in Sec. 4.1; These are filled with a medium with $(\epsilon_S,\ \epsilon_\infty,\ \sigma,\ \tau_D) = (5.76,\ 1.5,\ 7{\times}10^{-4}\,\mathrm{S/m},\ 7\,\mathrm{ps})$. When a propagation speed at 50 GHz is used for the determination of $\Delta t_{\mathrm{CFLlossy}}$, $\Delta t_{\mathrm{CFLlossy}}$ equals $\sqrt{2.23} \times \Delta t_{\mathrm{CFLlossless}}$ because the relative permittivity of the medium at 50 GHz is $2.23{+}j1.61$. The receivers are located within 15 Δs of the source which, for the limited recorded time, realizes a free space simulation. An error function is defined as $\mathcal{S}_e = \sqrt{\dfrac{\sum_f |\mathcal{S}_{FDADI}(f) - \mathcal{S}_{FDFD}(f)|^2}{\sum_f |\mathcal{S}_{FDFD}(f)|^2}}$ where $\mathcal{S}_{FDADI}(f)$ and $\mathcal{S}_{FDFD}(f)$ are the frequency spectrums of the signal received in FD-ADI-FDTD and FD-FDTD, respectively. The average error across the observation points is shown in Fig. 3 with $N_{CFL} = 1 \sim 10$. As a comparison, the error for a lossless case is also plotted. Note that the error is below 0.1 when $N_{CFL} \leq 6$ for both lossless and lossy cases. The errors from lossy and lossless cases are almost identical. This suggests that the error for the lossy case with Δt can be estimated from the error for the lossless case with $(v/v_h)\ \Delta t$. v_h is calculated from the media parameters and the frequency showing about -60 dB attenuation relative to the mainlobe of the source excitation.

It is concluded from Fig. 3 and Fig. 1 that those applications which accommodate an error higher than 0.1 gain a time benefit from FD-ADI-FDTD by using $N_{CFL} \geq 6$.

5 Conclusions

A detailed numerical formulation of FD-ADI-FDTD was given, including **D** field source excitation. A method of dealing with the CFL stability condition in a lossy medium for UWB systems was given, utilizing the frequency spectrum of the source excitation.

The error in the lossy case was proved to equal the lossless case with an appropriate N_{CFL} adjustment. It is shown that FD-ADI-FDTD is applicable for problems which can accommodate error higher than 0.1 with $N_{CFL} \geq 6$, gaining a simulation time benefit over FD-FDTD.

DOI: 10.1587/elex.1.528
Received October 29, 2004
Accepted November 08, 2004
Published December 10, 2004